J. Fluid Mech. (2013), *vol.* 714, *pp.* 190–212. © Cambridge University Press 2013
doi:10.1017/jfm.2012.466

Influence of low-frequency vibration on thermocapillary instability in a binary mixture with the Soret effect: long-wave versus short-wave perturbations

Irina S. Fayzrakhmanova[1,2,3], Sergey Shklyaev[4,3]† and Alexander A. Nepomnyashchy[1,5]

[1]Department of Mathematics, Technion – Israel Institute of Technology, Haifa 32000, Israel

[2]Department of General Physics, Perm State Technical University, Perm 614990, Russia

[3]Institute of Continuous Media Mechanics, Ural Branch of Russian Academy of Sciences, Perm 614013, Russia

[4]Department of Chemical Engineering, University of Puerto Rico – Mayagüez, Mayagüez, PR 00681, USA

[5]Minerva Center for Nonlinear Physics of Complex Systems, Technion – Israel Institute of Technology, Haifa 32000, Israel

(Received 27 January 2012; revised 5 August 2012; accepted 18 September 2012)

We study the influence of low-frequency vibration on Marangoni instability in a layer of a binary mixture with the Soret effect. A linear stability analysis is performed numerically for perturbations of a finite wavelength (short-wave perturbations). Competition between long-wave and short-wave modes is found: the former ones are critical at smaller absolute values of the Soret number χ, whereas the latter ones lead to instability at higher $|\chi|$. In both cases the vibration destabilizes the layer. Two variants of calculations are performed: via Floquet theory (linear asymptotic stability) and taking noise into consideration (empirical criterion). It is found that fluctuations substantially reduce the domains of stability. Further, while studying a limiting case within the empirical criterion, we have found a short-wave instability mode overlooked in former investigations of coupled Rayleigh–Marangoni convection in a layer of pure liquid.

Key words: Marangoni convection, parametric instability

1. Introduction

Thermal buoyancy or surface-tension-driven convection under modulated conditions has been investigated in a number of works (Gershuni & Lyubimov 1998). These works deal with such processes as vibration, temperature oscillations, periodic boundary motion: below, for the sake of brevity, we call these actions ‘external forcing’, without further specification. The well-developed and widely used Floquet method is quite appropriate for exploring stability of a system. Floquet multipliers

† Email address for correspondence: shklyaev@yandex.ru

https://doi.org/10.1017/jfm.2012.466 Published online by Cambridge University Press

allowing us to infer whether the perturbation grows at large time scale can be calculated, tracking the evolution of a perturbation during a period of modulation.

In the limit of low modulation frequency, the Wentzel–Kramers–Brillouin (WKB) approximation (Nayfeh 1973) makes possible a further simplification of the analysis. Due to the large difference between the modulation period and the time scale inherent to the system, an instantaneous growth rate can be introduced. Indeed, the modulation is so slow that the system has enough time to relax before changing the momentary value of the external forcing. Consequently, one only has to solve the linear problem with constant (frozen) coefficients at each time step. In order to trace the evolution of a perturbation during a modulation period Floquet theory can again be applied. The Floquet multiplier is given by the integral of the instantaneous growth rate over the period of modulation. At the stability boundary the perturbation grows during part of the period and decays during the rest of the period, remaining at the same amplitude overall. Following Homsy (1974) we name it the *asymptotic stability* criterion. It has been successfully applied to many convective problems: see, for instance, Rosenblat & Herbert (1970), Myznikova & Smorodin (2001), Or (2001), Smorodin, Myznikova & Keller (2002) and Myznikova & Smorodin (2009).

However, experimental studies (Finucane & Kelly 1976) and numerical calculations (Homsy 1974; Finucane & Kelly 1976; Lyubimov, Lyubimova & Maryshev 2010) clearly demonstrated that this edifice was flawed, leading to overestimation of the stability boundary. The main reason for such an effect is the implicit assumption that the system is initially perturbed and no other perturbations appear in the course of further evolution. However, noise, which is present in real physical systems, can drastically change the dynamics. On one hand, during the subcritical part of the period, the exponential decay of the perturbation stops as soon as the perturbation becomes comparable to the noise level. On the other hand, at the supercritical time interval noise can provoke a large difference between the instantaneous state and the base state, whose stability is analysed. Owing to this distinction, the base state will be interpreted as unstable; moreover, even nonlinear effects can be important at this growth stage. The effects just mentioned are especially important for the low-frequency modulation, when the supercritical and subcritical time periods last rather long in comparison with the typical time scale of the system.

Generally speaking, this circumstance makes it difficult to formulate the stability criterion in noisy systems: such a criterion depends on the noise amplitude, system nonlinearity, and so on. However, it is possible to point out the lower boundary of stability, which manifests itself for a rather large amplitude of noise. This *strong global stability* (empirical) criterion was formulated by Homsy (1974): the system was treated as an unstable one as soon as a growing perturbation appears at some time instant. We emphasize once again that the criterion provides an overestimation of the instability domain.

Finucane & Kelly (1976) compared experimental results with both linear analysis and nonlinear computations. They also mentioned that at low frequencies it was difficult to distinguish between convection and conduction: the classification of the state was determined by the chosen criterion. The analytical and numerical studies performed by Lyubimov *et al.* (2010) for several nonlinear problems demonstrated that even under additive noise of small intensity, the empirical criterion agreed well with the stability threshold found numerically. In contrast, the asymptotic stability criterion resulted in a substantial overestimation of the stability boundary. Even the overall effect changed: destabilization of the base state was observed instead of stabilization as predicted by Floquet theory.

https://doi.org/10.1017/jfm.2012.466 Published online by Cambridge University Press

The paper by Fayzrakhmanova, Shklyaev & Nepomnyashchy (2010) investigated the influence of vibration on long-wave thermocapillary convection in a layer of a binary mixture with the Soret effect. The main purpose of the cited paper was to study the parametric excitation of the long-wave oscillatory convection (Oron & Nepomnyashchy 2004), a rare and still not fully explored phenomenon. Although the paper by Fayzrakhmanova *et al.* (2010) dealt with that particular problem, qualitatively similar results are expected for a wide class of problems where arbitrary periodic forcing is imposed on the system, admitting a long-wave oscillatory mode with the quadratic or more complicated dispersion relation. Other examples of such systems include: buoyancy convection in a two-layer system (Lyubimova & Parshakova 2007) or in a binary liquid layer (Pismen 1988); Marangoni convection in systems with a deformable free surface/interface, i.e. a two-layer (Nepomnyashchy & Simanovskii 2007) or one-layer (Shklyaev, Khenner & Alabuzhev 2010, 2012) system of pure liquid and a binary liquid layer (Podolny, Oron & Nepomnyashchy 2005, 2006; Bestehorn & Borcia 2010); mixed buoyancy and surface-tension-driven convection in a layer of a binary mixture (Podolny, Nepomnyashchy & Oron 2008, 2010).

The analysis of Fayzrakhmanova *et al.* (2010) demonstrated the incompleteness of the long-wave approach. It was found that in a certain domain of parameters the rescaled critical wavenumber tended to infinity, thus leaving the domain of applicability of long-wave approximation. Resolution of that difficulty is the primary motivation of the present paper, which contains the stability analysis with respect to disturbances with arbitrary wavenumbers.

Thus, the present work is devoted to the influence of the low-frequency vibration on a short-wave thermocapillary instability in a layer of a binary mixture with the Soret effect. The problem is solved numerically: both the above-mentioned stability criteria – the asymptotic stability and empirical ones – are applied. As noted above, the stability boundaries obtained by means of these two methods provide the upper and lower estimates, respectively, for stability in a real system. Again, we expect that qualitatively similar results (competition between long-wave and short-wave perturbations, various types of temporal evolution of critical perturbations, etc.) can be found in a wide class of problems.

The paper is organized as follows. We start with the problem formulation in § 2. In § 3 we describe a method we use to treat the linear problem. The numerical results are discussed in § 4 within the asymptotic stability criterion (§ 4.1) and empirical criterion (§ 4.2). As an important particular limiting case, in § 4.2.1 we consider coupled Rayleigh–Marangoni convection in the absence of vibration; we have found a short-wave monotonic mode for this problem which has not been previously reported. Results are summarized in § 5.

2. Problem statement

We consider an infinite layer of an isothermally incompressible binary mixture heated from below in the presence of the Soret effect. The lower rigid boundary $z_* = 0$ is subject to perpendicular oscillations with an amplitude b_* and a frequency Ω_*. (Starred variables hereafter refer to the dimensional quantities.) The vibration period is large in comparison with the characteristic time scales inherent to the diffusion of the mass, momentum and heat. The vibration amplitude b_* is assumed to be larger than the layer thickness d_* to ensure a finite impact of the vibration (see the discussion in the last paragraph of § 2). The upper free surface $z_* = d_*$ is non-deformable: thus no Faraday waves are generated by the vibration. That approximation is valid when

https://doi.org/10.1017/jfm.2012.466 Published online by Cambridge University Press

the Galileo number is large and the capillary number is small (in physical terms, the gravity and the surface tension are sufficiently strong). At the same time, the Rayleigh number is assumed to be small, i.e. the buoyancy is disregarded. An example of a physical system where all the above-mentioned restrictions on the amplitude and frequency of vibration are valid and no Faraday's instability appears, is given in appendix A of the paper by Fayzrakhmanova *et al.* (2010). Both the solid wall and ambient gas are of low thermal conductivity with respect to that of the binary mixture. In the absence of the motion, a transverse temperature gradient $-a_*$ is held throughout the layer, which, in turn, induces a gradient of solute concentration owing to the Soret effect and no-penetration conditions for the solute at $z_* = 0, d_*$. The mass flux is given by the relation

$$\boldsymbol{J}_m = -\rho_* D_* (\boldsymbol{\nabla} C_* + \alpha_* \boldsymbol{\nabla} T_*), \tag{2.1}$$

where ρ_*, D_*, α_*, T_* and C_*, are the density of the liquid, mass diffusivity, Soret coefficient, temperature and solute concentration, respectively.

The surface tension σ_* and density ρ_* depend linearly on both the temperature and solute concentration:

$$\sigma_* = \sigma_0 - \sigma_T (T_* - T_*^0) + \sigma_C (C_* - C_*^0), \tag{2.2}$$

$$\rho_* = \rho_0 - \beta_T (T_* - T_*^0) - \beta_C (C_* - C_*^0), \tag{2.3}$$

wherein T_*^0 (C_*^0) is the reference value of T_* (C_*), $\sigma_T = -\partial\sigma_*/\partial T_*$, $\sigma_C = \partial\sigma_*/\partial C_*$; β_C and β_T are the solutal and thermal expansion coefficients, respectively.

The problem under consideration admits the base solution, corresponding to the conductive distributions of both the temperature and concentration in a motionless liquid. In dimensionless form (we use κ_*/d_*, d_*^2/κ_*, d_*, $a_* d_*$, $\sigma_T a_* d_*/\sigma_C$ and $\rho_0 \nu_* \kappa_*/d_*^2$ as the scales for the velocity, time, length, temperature, solute concentration and pressure, respectively, where κ_* is the thermal diffusivity and ν_* is the kinematic viscosity), this base state has the form

$$\boldsymbol{v}_b = 0, \quad T_b = -z + T_{00}, \quad C_b = \chi z + C_{00}, \quad p_b = \frac{b}{2}(\varphi_\chi z^2 + p_{01} z)\cos\omega t + p_{00}, \tag{2.4}$$

where the constants T_{00}, C_{00}, p_{01} and p_{00} are unimportant for the further analysis, and $\varphi_\chi \equiv \varphi\chi - 1$; χ and φ are the Soret and modified separation number, respectively:

$$\chi = \frac{\alpha_* \sigma_C}{\sigma_T}, \quad \varphi = \frac{\beta_C \sigma_T}{\beta_T \sigma_C}. \tag{2.5}$$

Note that φ, in contrast to the true separation number, determines the respective importance of volumetric and surface effects.

Below we consider the stability of this base state. Owing to obvious symmetry reasons, the three-dimensional stability problem can be reduced to the two-dimensional one. The streamfunction ψ is introduced according to the relations $w = -\partial_x \psi$, $u = \partial_z \psi$, where u and w are the x- and z-components of the fluid velocity. We separate the dependence on x from the dependence on the other variables using the ansatz

$$g(t, x, z) = \mathrm{e}^{\mathrm{i}kx} \tilde{g}(t, z), \quad g = (\psi, T, C) \tag{2.6}$$

https://doi.org/10.1017/jfm.2012.466 Published online by Cambridge University Press

with a wavenumber k. Thus, the dynamics of small two-dimensional perturbations is governed by the following boundary value problem:

$$\frac{\partial \Delta\tilde{\psi}}{\partial t} = P(\Delta^2\tilde{\psi} - \mathrm{i}k(\tilde{T} + \varphi\tilde{C})b\cos\omega t), \tag{2.7a}$$

$$\frac{\partial \tilde{T}}{\partial t} = -\mathrm{i}k\tilde{\psi} + \Delta\tilde{T}, \tag{2.7b}$$

$$\frac{\partial \tilde{C}}{\partial t} = \mathrm{i}k\chi\tilde{\psi} + L\Delta(\tilde{C} + \chi\tilde{T}), \tag{2.7c}$$

$$\tilde{\psi} = \partial_z\tilde{\psi} = \partial_z\tilde{T} = \partial_z\tilde{C} = 0 \quad \text{at } z = 0, \tag{2.7d}$$

$$\tilde{\psi} = \partial_z\tilde{T} = \partial_z\tilde{C} = 0, \quad \partial_z^2\tilde{\psi} = -\mathrm{i}kM(\tilde{T} - \tilde{C}) \quad \text{at } z = 1. \tag{2.7e}$$

Here $\Delta \equiv \partial_z^2 - k^2$. According to (2.7$d$) and (2.7$e$) both the boundaries are insulated for thermal perturbations and impermeable for the solute. Influence of a heat flux from the free surface was considered by Fayzrakhmanova, Shklyaev & Nepomnyashchy (2011).

In addition to the above-mentioned Soret and modified separation numbers, five dimensionless parameters enter into (2.7):

$$P = \frac{\nu_*}{\kappa_*}, \quad L = \frac{D_*}{\kappa_*}, \quad M = \frac{\sigma_T a_* d_*^2}{\nu_*\rho_0\kappa_*}, \quad b = \frac{b_*\Omega_*^2 d_*^4\beta_T a_*}{\kappa_*\nu_*}, \quad \omega = \frac{\Omega_* d_*^2}{\kappa_*}, \tag{2.8}$$

which are the Prandtl, Lewis and Marangoni numbers, and the amplitude and frequency of vibration, respectively.

This problem was recently analysed in the long-wave approximation ($k \ll 1$) for the low frequency $\omega \ll \min(1, P, L)$, when the frequency of vibration is comparable to the eigenfrequency of the long-wave oscillatory mode (Fayzrakhmanova *et al.* 2010). The former restriction is relaxed in the present paper, whereas the latter one is kept.

It should be emphasized that for $\omega \ll 1$, the amplitude b can be presented as a product of two small parameters, $\beta_T a_* d_*$ and $P\omega^2$, and the ratio b_*/d_*. It is clear that the latter parameter has to be large in order to provide finite values of b. Otherwise, vibration produces only small corrections to the stability thresholds found by Oron & Nepomnyashchy (2004).

3. Method of solution

3.1. *Low-frequency expansion*

At small ω the WKB method (Nayfeh 1973) is appropriate for the study of linear stability. Introducing a new variable $\tau = \omega t$, we represent the solution of (2.7) as follows:

$$\tilde{g} = \exp(\omega^{-1}\Psi(\tau))(g_0 + \omega g_1 + \cdots), \tag{3.1}$$

where again $\tilde{g}$ is each of the perturbation fields $(\tilde{\psi}, \tilde{T}, \tilde{C})$, and Ψ is an analogue of the eikonal function in geometric optics (Nayfeh 1973). Substituting this ansatz into (2.7) and expanding Ψ in powers of ω,

$$\Psi = \Psi_0 + \omega\Psi_1 + \cdots, \tag{3.2}$$

https://doi.org/10.1017/jfm.2012.466 Published online by Cambridge University Press

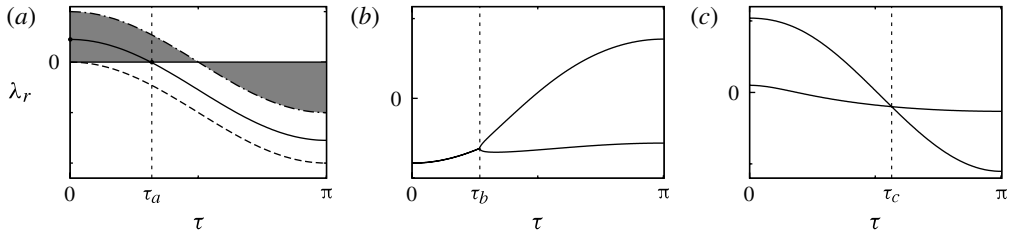


FIGURE 1. A schematic representation of time variation of the real part of the growth rate. (*a*) Case I: no intersection of the growth rate belonging to different modes occurs during the period. The dot-dashed, dashed and solid lines correspond to the case of zero noise level ($M_0(k)$, see (3.8), i.e. the areas of the filled domains are equal to each other), finite noise level ($M_\infty(k)$, see (3.13)) and small noise level ($M_\delta(k)$, see (3.12)), respectively. In the third case τ_a is determined by (3.10). (*b*) Case II: an oscillatory mode is split into a pair of monotonic modes at certain $\tau = \tau_b$. (*c*) Case III: there is an intersection of λ_r for two different modes at certain $\tau = \tau_c$. Corresponding values of λ_i are different at that time instant.

to leading order we arrive at the problem

$$\lambda\Delta\psi_0 = P(\Delta^2\psi_0 - \mathrm{i}k(T_0 + \varphi C_0)b\cos\tau), \tag{3.3a}$$

$$\lambda T_0 = \Delta T_0 - \mathrm{i}k\psi_0, \tag{3.3b}$$

$$\lambda C_0 = L\Delta(C_0 + \chi T_0) + \mathrm{i}k\chi\psi_0, \tag{3.3c}$$

$$\psi_0 = \partial_z\psi_0 = \partial_z T_0 = \partial_z C_0 = 0 \quad \text{at } z = 0, \tag{3.3d}$$

$$\psi_0 = \partial_z T_0 = \partial_z C_0 = 0, \quad \partial_z^2\psi_0 = -\mathrm{i}kM_0(T_0 - C_0) \quad \text{at } z = 1, \tag{3.3e}$$

where $\lambda(\tau) = \mathrm{d}\Psi_0/\mathrm{d}\tau$. As can be expected, at any fixed τ (3.3) coincides with the stability problem for the quiescent state in a heated layer of a binary fluid in the presence of both buoyancy and Marangoni effects and in the absence of vibration. Within this analogy the instantaneous acceleration of vibration $b\cos\tau$ plays the role of the Rayleigh number, whereas $\lambda(\tau)$ is the momentary growth rate. (Keeping this in mind, we term λ as a 'growth rate' below.) Indeed, since the vibration period is very large, there is enough time for a relaxation of a perturbation before a substantial change in the acceleration occurs.

At fixed 'Rayleigh number' $b\cos\tau$ the boundary value problem (3.3) is reduced to the limiting case $Bi = 0$ (zero heat flux from the free surface) of the problem studied by Podolny *et al.* (2008, 2010) for small and finite k, respectively.

3.2. *Floquet theory*

In order to consider an initially introduced perturbation we apply Floquet theory, thus calculating the mean value of the growth rate during a vibration period.

The three different situations shown in figure 1 are possible. In Case I there is no merging or crossing of eigenvalues by changing τ (see the dot-dashed line in figure 1*a*), each eigenmode $g_0 = (\psi_0, T_0, C_0)$ and the corresponding eigenvalue λ depend periodically on the parameter τ due to the factor $b\cos\tau$ in (3.3). The growth of the disturbance during the period of vibration, according to (3.1), is determined by the expression

$$\Psi_r(\pi) - \Psi_r(-\pi) = \int_{-\pi}^{\pi} \lambda_r(\tau)\,\mathrm{d}\tau. \tag{3.4}$$

https://doi.org/10.1017/jfm.2012.466 Published online by Cambridge University Press

Hereafter subscripts r and i denote the real and imaginary part of the corresponding expression, respectively. In fact, since only the term with $\cos\tau$ appears in (3.3), which is an even function of τ, one can calculate the integral over the vibration half-period, $0 < \tau < \pi$, arriving at

$$\Psi_r(\pi) = \int_0^\pi \lambda_r(\tau)\,\mathrm{d}\tau. \tag{3.5}$$

Hereafter we set $\Psi(0) = 0$. As a matter of fact, to find the stability boundary in Case I it is sufficient to calculate the integral only for the mode with the maximum value of λ_r, which provides

$$\Psi_r(\pi) = \int_0^\pi \max_n\{\lambda_{nr}(\tau)\}\,\mathrm{d}\tau. \tag{3.6}$$

(The subscript n enumerates the branches of the eigenmodes.)

In Case II, a pair of complex conjugate eigenvalues is transformed into a pair of real eigenvalues at a certain time instant $\tau = \tau_b$ during the vibration period: see figure 1(*b*). The solution, which is a superposition of two complex eigenfunctions with complex conjugate amplitudes at $\tau < \tau_b$, has to be projected at $\tau > \tau_b$ on the two-dimensional manifold formed by two real eigenfunctions. The amplitude of critical (with larger λ) monotonic mode comprises a certain part μ ($|\mu| < 1$) of the amplitude of the oscillatory mode (the remaining part of the amplitude belongs to the faster decaying mode with the smaller λ). The factor μ is unknown and is determined by subtle details such as the evolution of the phase of oscillations by crossing the point $\tau = \tau_b$, as shown in appendix A. Fortunately, this factor (unless it is very small) provides only an $O(\omega)$ correction to the growth rate, therefore to leading order the decay (growth) of the perturbation is again determined by (3.6).

Finally, in Case III at $\tau = \tau_c$ there is an intersection of λ_r for a pair of modes with different λ_i: see figure 1(*c*). As shown in appendix B, in that case there is no coupling between the two modes and one has to choose the branch providing the maximal gain in the 'eikonal' function, i.e.

$$\Psi_r(\pi) = \max\left\{\int_0^\pi \lambda_{1r}(\tau)\,\mathrm{d}\tau,\ \int_0^\pi \lambda_{2r}(\tau)\,\mathrm{d}\tau\right\}, \tag{3.7}$$

where subscripts 1 and 2 enumerate the competing modes.

Consequently, in all three cases the stability boundary is determined by the integral relation

$$\Psi_r(\pi) = 0, \tag{3.8}$$

where $\Psi_r(\pi)$ is determined by either (3.6) (Cases I and II) or (3.7) (Case III).

During part of the vibration period the perturbation grows, then it decays and the absolute value of the Floquet multiplier, $\exp(\omega^{-1}\Psi_r(\pi))$, is equal to unity at the stability boundary: see the dot-dashed line in figure 1(*a*). This stability condition determines the neutral stability curve $M_0(k)$ with the other parameters kept fixed.

Depending on values of $\Psi_i(\pi) = \int_0^\pi \lambda_i\,\mathrm{d}\tau$, we refer to the stability modes as 'synchronous' when the corresponding value is zero, or 'quasiperiodic' otherwise. Note that in the former case this classification is inexact, because $\Psi_i(\pi) = 0$ only annihilates the leading ($O(\omega^{-1})$) part of the phase, although an $O(\omega)$ correction to λ_i can provide a finite phase. Therefore the synchronous mode can in fact be subharmonic or quasiperiodic or a true synchronous mode. In contrast, for $\Psi_i(\pi) \neq 0$ a quasiperiodic mode takes place.

https://doi.org/10.1017/jfm.2012.466 Published online by Cambridge University Press

3.3. *Finite level of noise*

Applying the stability condition (3.8) we consider an asymptotic stability (Homsy 1974), thus dealing with an idealistic situation when an initial perturbation decays exponentially without any lower boundary, at a stage when $\lambda_r^{(m)}(\tau) = \max_n\{\lambda_{nr}(\tau)\} < 0$. However, in a realistic situation, such a lower boundary is determined by a noise level δ; the perturbation smaller (in a certain sense) than δ no longer decays. (It is assumed that the non-decaying perturbation is generated by a stochastic external force.) In that case, an experimenter will observe a certain motion (and hence report on the 'instability' of the quiescent state) if, at least during some part of the period of modulation, the noise of order δ is amplified to the measurable level $O(1)$. Consequently, in the presence of noise the meaning of the notion 'stability' is changed. Instead of using the standard notions accepted in the theory of dynamical systems, we shall call the system 'unstable' if the noise of order δ is amplified to the level $O(1)$. As is well known (Finucane & Kelly 1976), this 'empirical' criterion of the stability is especially important in the limit of low frequency. Indeed, in this limit a perturbation has enough time to grow (or even to establish a new regime) when $\lambda_r^{(m)} > 0$.

Let us find the criterion of the noise amplification in the case of a low-frequency gravity modulation. Consider a disturbance characterized by a certain wavenumber k. For sufficiently small M, the maximum growth rate $\lambda_r^{(m)}(k, M, \tau)$ is negative during the whole period $-\pi \leqslant \tau \leqslant \pi$, and the noise is not amplified. Let $M_\infty(k)$ denote the value of M such that $\lambda_r^{(m)}(k, M, \tau)$ becomes equal to zero at a certain value of τ. It is intuitively clear that the growth rate achieves its maximum at either maximum or minimum values of the 'Rayleigh number' $R = b\cos\tau$, i.e. at $\tau = 0$ (see the dashed line $\lambda_r^{(m)}(\tau)$ in figure 1*a*) or $\tau = \pi$; this guess is confirmed numerically. Without loss of generality, we assume that the maximum growth rate is achieved at $\tau = 0$ (and hence $\lambda_r^{(m)}$ grows as R increases). For $M = M_\infty + \Delta M$ slightly above the threshold M_∞ (hereafter we assume that $\Delta M > 0$, so that $\lambda_r^{(m)}$ is enhanced by the increase in the Marangoni number), the growth rate can be estimated as

$$\lambda_r^{(m)} \approx \frac{\partial\lambda_r^{(m)}}{\partial M}\Delta M - \frac{\partial\lambda_r^{(m)}}{\partial R}b\frac{\tau^2}{2}, \tag{3.9}$$

where both the partial derivatives are calculated at $M = M_\infty$ and $R = b$. Thus, $\lambda_r^{(m)}$ is positive during the time interval $-\tau_a < \tau < \tau_a$, where $\lambda_r^{(m)}(\tau_a) = 0$, i.e.

$$\tau_a^2 \approx 2\frac{\partial\lambda_r^{(m)}}{\partial M}\Delta M\left(\frac{\partial\lambda_r^{(m)}}{\partial R}b\right)^{-1}. \tag{3.10}$$

During that time interval, the disturbance grows from δ to

$$\delta\exp\left(\frac{1}{\omega}\int_{-\tau_a}^{\tau_a}\lambda_r^{(m)}\,\mathrm{d}\tau\right) \sim \delta\exp\left(\frac{(\Delta M)^{3/2}}{\omega}\right). \tag{3.11}$$

Therefore, the noise is amplified to the level of $O(1)$ if

$$\Delta M = M_\delta - M_\infty \sim (\omega|\ln\delta|)^{2/3} \tag{3.12}$$

(see the solid line in figure 1*a*). Thus, one can see that only at a very low level of noise, $\delta \sim \exp(-\omega^{-1})$, $\Delta M = O(1)$. If $\delta \gg \exp(-\omega^{-1})$, we find that $\Delta M = o(1)$ in the limit $\omega \ll 1$, and we can use the relation

$$\max_{0\leqslant\tau\leqslant\pi}\lambda_r^{(m)}(k, M, \tau) = 0, \tag{3.13}$$

https://doi.org/10.1017/jfm.2012.466 Published online by Cambridge University Press

as the criterion of 'instability' (in the meaning discussed above). In some sense this criterion corresponds to the *amplitude criterion* suggested by Rosenblat & Herbert (1970).

Below we deal with the two opposite cases, either $\delta = 0$ (§ 4.1) or $\exp(-\omega^{-1}) \ll \delta \ll 1$ (§ 4.2), which are called 'absence of noise' (asymptotic stability criterion) and 'finite level of noise' (empirical criterion), respectively. It is clear that these calculations provide the upper and lower boundaries, respectively, for the stability conditions. It is noteworthy that for most practically valid situations the stability threshold should be close to M_∞ because of its weak (logarithmic) dependence on the noise intensity δ: see (3.12).

In contrast to the noise-free system, at $\delta \gg \exp(-\omega^{-1})$ the system, generally speaking, leaves the vicinity of the base state during the first period (or the first few periods) of vibration. Therefore the perturbations should be classified as oscillatory and monotonic (rather than quasiperiodic and synchronous) depending on $\lambda_i^{(m)}(\tau = 0, \pi)$. Again, for the monotonic mode one only ensures that the fast oscillations are absent, though the perturbation can oscillate due to $O(\omega)$ corrections to $\lambda_i^{(m)}$.

It should be emphasized that the value of M_∞ corresponds to the limiting case $Bi = 0$ of the problem considered by Podolny *et al.* (2008, 2010). However, their results cannot be directly used in our case because of a different parameter range. First of all, most of the computations in the above-mentioned papers have been carried out for positive values of the Bond number (which is the ratio of the Rayleigh and Marangoni numbers), whereas in our case $b\cos\tau$ changes its sign during the vibration period. Also, keeping in mind nanofluidic applications, the Lewis number was set asymptotically small in the paper by Podolny *et al.* (2010). Therefore, we have to perform additional computations for appropriate values of parameters. Our results on the long-wave instability (see (4.9), (4.10) below), as well as on the transition from the long-wave instability to short-wave instability, agree with those obtained by Podolny *et al.* (2008, 2010) up to notations.

For numerical computation of λ for both $\delta = 0$ and $\delta \gg \exp(-\omega^{-1})$, we use the shooting method.

4. Results

In the numerical analysis presented below we fix a pair of parameters, $\varphi = 1$ and $L = 0.01$, in order to compare the obtained results with the computations performed within the long-wave limit (see Fayzrakhmanova *et al.* 2010). (It is worth noting that the sign of φ determines only the sign of $\beta_C\sigma_C$ because both β_T and σ_T are usually positive. Therefore χ can be either positive or negative depending on signs of both the Soret coefficient α_D and σ_C.) For the same reason, we mainly use $b = 160$ in computations; some calculations in § 4.2 are performed for $b = 80$. According to appendix A of the paper by Fayzrakhmanova *et al.* (2010), these values of the amplitude correspond to $b_* \sim 10^2$ cm at $\Omega_* = 0.1$ rad s^{-1} for a layer of thickness 0.03 cm of water–ethanol mixture. In contrast to the long-wave limit, the problem under consideration is characterized by the Prandtl number as well; in computation we set $P = 2$. The Soret number χ is varied in a wide range to obtain the stability boundaries M_0 and M_∞. Further, at the end of §§ 4.1 and 4.2 we briefly discuss the variation of the corresponding stability boundaries with both φ and P. The Lewis number is kept fixed because its value is typical for many binary liquids. Finally, the value of the amplitude b is chosen to be rather large (maybe even so large that

https://doi.org/10.1017/jfm.2012.466 Published online by Cambridge University Press

the Faraday instability emerges) since for any smaller values of b the stability maps are qualitatively similar to those shown below. Therefore, the computations provide a typical picture which can be observed experimentally.

4.1. *Zero level of noise*

4.1.1. *Small k*

We start the discussion of the results with the noise-free system, when the average value of the growth rate vanishes at the stability boundary $M = M_0(k)$ (see (3.8), the dot-dashed line in figures 1*a*, 1*b* and 1*c*).

As we have stated above, the long-wave instability within (2.7) was studied by Fayzrakhmanova *et al.* (2010). To that end the rescaled wavenumber $K = k/\sqrt{\omega}$ was introduced in the cited paper and competition between three instability modes was found. These modes are: (i) the long-wave synchronous mode with $K = 0$; (ii) the subharmonic mode with a certain finite critical value of K; and (iii) the short-wave synchronous mode, when the critical Marangoni number is reached at $K \to \infty$. Below, for the sake of brevity, we term these modes as (i) true long-wave (TLW), (ii) subharmonic (SH) and (iii) intermediate long-wave (ILW) modes.

The last case is intimately connected with the problem under consideration, providing a matching of long-wave results and the analysis of true short-wave perturbations. Indeed, large values of K correspond to the long-wave approximation ($k \ll 1$) within (3.3), i.e. the results for the ILW mode are valid at small k. It is shown in Section IVC of the cited paper (see (72) in Fayzrakhmanova *et al.* 2010) that the growth rate λ for ILW solves the following quadratic equation:

$$\lambda^2 = k^2\lambda\xi_1 + k^4\xi_2, \quad \xi_1 = \alpha - \varphi_\chi A\cos\tau, \quad \xi_2 = \Theta + \Phi A\cos\tau, \tag{4.1}$$

where $\alpha = (\chi+1)M/48 - L - 1$, $\Theta = \chi_L M/48 - L$, $\Phi = -\varphi_\chi(L+1) - 1$, $\chi_L = \chi + L + \chi L$ and $A = b/320$. Recall that $\varphi_\chi = \varphi\chi - 1$.

This equation obviously has either real or complex solutions, allowing additional classification of the ILW modes as synchronous (ILW-S: λ is real during the whole period) and quasiperiodic modes (ILW-Q: λ is complex at least during part of a period), respectively. Note that the ILW-Q mode is not critical according to Fayzrakhmanova *et al.* (2010): the SH mode sets in instead.

In the absence of noise, the integral which appears in (3.8) is a cumbersome function including elliptic integrals of the first and second kinds, and $M_0(k = 0)$ can be found only numerically. The only case when some analytical progress is possible is that where the discriminant $\xi_1^2 + 4\xi_2$ for (4.1) is negative during the whole period of oscillations. It is obvious that in this case $\lambda_r = k^2\xi_1/2$, i.e. the stability threshold is determined by

$$M = 48\frac{1+L}{1+\chi}, \tag{4.2}$$

which is in fact the stability threshold for the long-wave oscillatory mode in the absence of vibration (Oron & Nepomnyashchy 2004). The discriminant is negative under the following condition:

$$-\frac{\chi(1+L+L^2)+L^2}{1+\chi} > |\Phi|A + \frac{\varphi_\chi^2 A^2}{4}. \tag{4.3}$$

For $A = 0$, (4.3) coincides with the condition of existence for the long-wave oscillatory mode (the left-hand side can be viewed as the squared frequency of the oscillations up

https://doi.org/10.1017/jfm.2012.466 Published online by Cambridge University Press

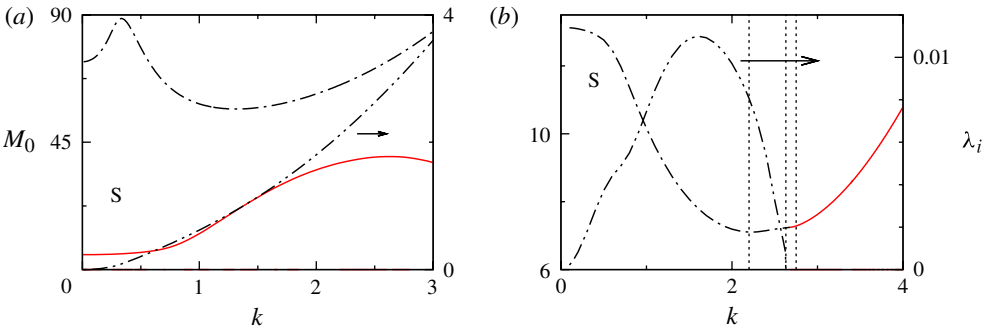


FIGURE 2. (Colour online) Neutral stability curves $M_0(k)$ at $b = 160$ (left axis) and the frequency of neutral perturbations for the quasiperiodic mode (right axes, dot-dot-dashed lines). The solid and dot-dashed lines correspond to the synchronous and quasiperiodic modes, respectively. The stability domains are marked 'S'. (*a*) $\chi = -0.34$; (*b*) $\chi = 0.11$. The vertical lines in (*b*) mark three values of k for those $\lambda(\tau)$ presented in figure 3.

to the factor k^4). For any non-zero A, (4.3) imposes a stronger restriction on χ, since its right-hand part is obviously positive.

4.1.2. *Finite k*

In figure 2 typical neutral stability curves $M_0(k)$ are presented. One can see that at the negative values of the Soret number (see figure 2*a*) both synchronous and quasiperiodic modes exist simultaneously; the stability domain is situated between the corresponding curves. The quasiperiodic mode originates from the oscillatory mode found in the absence of the vibration (Shklyaev, Nepomnyashchy & Oron 2009). Similarly to the case $b = 0$ the neutral stability curve for the quasiperiodic mode comprises two parts with their own minima. One of them, at $k = 0$, is local for the chosen value of χ; (4.2) is valid in this case. The global minimum occurs for finite k. Therefore, the critical mode, similarly to the case $b = 0$, corresponds to formation of an oscillatory concentration boundary layer near the free surface: the solute being advected to this layer diffuses to the free surface and triggers an intensive solutal convection (see details in Shklyaev *et al.* 2009). Vibration as a volumetric effect is almost unimportant for that mode. With a decrease in $|\chi|$ the competition between these two minima occurs and at rather small $|\chi|$ the long-wave mode becomes critical. (However, the ILW-Q mode is critical only within the WKB theory: see the remark below.) Note that the value of the Soret number, which corresponds to this transition from the short-wave quasiperiodic mode to the ILW-Q mode, is smaller in the presence of vibration. Indeed, with increase in χ the inequality (4.3) becomes invalid and vibration strongly diminishes the Marangoni number for the ILW-Q mode. A typical dependence of $\lambda(\tau)$ for the quasiperiodic mode is given by figure 1(*c*), i.e. Case III takes place.

The synchronous mode stems from the monotonic mode found at $b = 0$ by Oron & Nepomnyashchy (2004). In the absence of vibration M_0 is negative; the change of sign for the critical Marangoni number with the growth of the vibration amplitude was found by Fayzrakhmanova *et al.* (2010). Qualitatively this vibration-induced destabilization ensues from the emergence of buoyancy convection at $\pi/2 < \tau < \pi$, when the vibration acceleration is directed towards the free surface and hence opposite to the both thermal- and concentration-induced density gradients. With decrease in $|\chi|$ the critical value of k diminishes, and again the long-wave mode (the ILW-S mode in

https://doi.org/10.1017/jfm.2012.466 Published online by Cambridge University Press

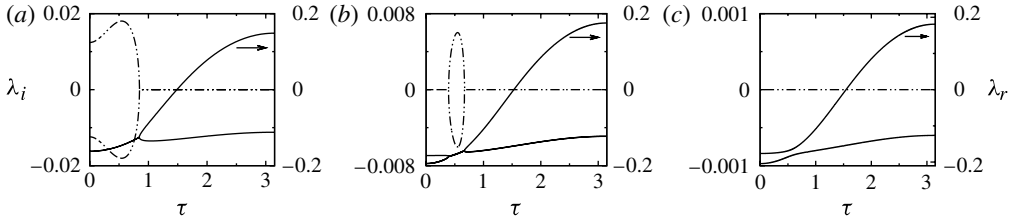


FIGURE 3. Variation of growth rate with the rescaled time τ at $b = 160$, $\chi = 0.11$ and (a) $k = 2.2$, (b) $k = 2.63$ and (c) $k = 2.75$; see the vertical lines in figure 2(b). $M_0 = 7.11, 7.23$ and 7.28, respectively.

this case) becomes critical. Note that the critical Marangoni number decreases fast for the long-wave perturbations, i.e. the stability domain is augmented by a decrease in $|\chi|$.

It is clear from figure 2(a) that the maximum value of $M_0(k)$ for the synchronous mode is close to the minimum value for the quasiperiodic mode. Further increase in $|\chi|$ leads to the overlap of the corresponding domains of instability at $\chi < -0.395$. Therefore, under this condition the layer is unstable for any value of M. (In fact, the threshold value of $|\chi|$ is even less: see below.)

In figure 2(b) the neutral stability curve at $\chi = 0.11$ is presented. It is clear that with the increase in the wavenumber the quasiperiodic mode alternates with the synchronous mode. A further increase in the Soret number makes the synchronous mode critical.

In order to illustrate switching between the quasiperiodic and synchronous modes, we demonstrate in figure 3 the variation of the growth rate with τ for three values of k. The qualitative change of the spectrum takes place with increase in k, when the oscillatory mode (Case II, figures 3a and 3b) is replaced with a pair of monotonic modes (Case I, figure 3c). The necessity to track the maximum value of $\lambda_r(\tau)$ considerably increases the computation time in such cases. It is also clear from figure 3 that both the quasiperiodic and synchronous modes at positive χ are in a close relation to the monotonic mode studied by Oron & Nepomnyashchy (2004) and Shklyaev *et al.* (2009) for small and finite k, respectively. However, with increase in the amplitude of vibration this mode can couple with another monotonic mode, giving rise to oscillations.

In figure 4(a) one can see the stability domain in the plane (χ, M_{0c}) at $b = 160$. A comparison with the results for the long-wave approximation (Fayzrakhmanova *et al.* 2010) is performed. It can be readily seen that the stability domain shrinks considerably in the presence of the short-wave perturbations; this effect is especially pronounced for larger $|\chi|$. For instance, the above-mentioned full destabilization of the layer at $\chi < -0.395$ does not exist within the long-wave approximation. However, all the long-wave modes remain critical within some intervals of χ. The especially important mode is SH, which is critical for negative χ instead of two competing quasiperiodic modes, a short-wave mode and the ILW-Q mode: see the dashed line and the dot-dashed lines in figure 4(a). As a result, the complete destabilization of the layer appears at $\chi < -0.374$, when the dashed and dotted lines intersect in figure 4(a). Other long-wave modes play an important role at small $|\chi|$: see figure 4(b).

The critical wavenumber and frequency are demonstrated in figures 4(c) and 4(d), respectively. The discontinuities in both dependences as well as the derivative

https://doi.org/10.1017/jfm.2012.466 Published online by Cambridge University Press

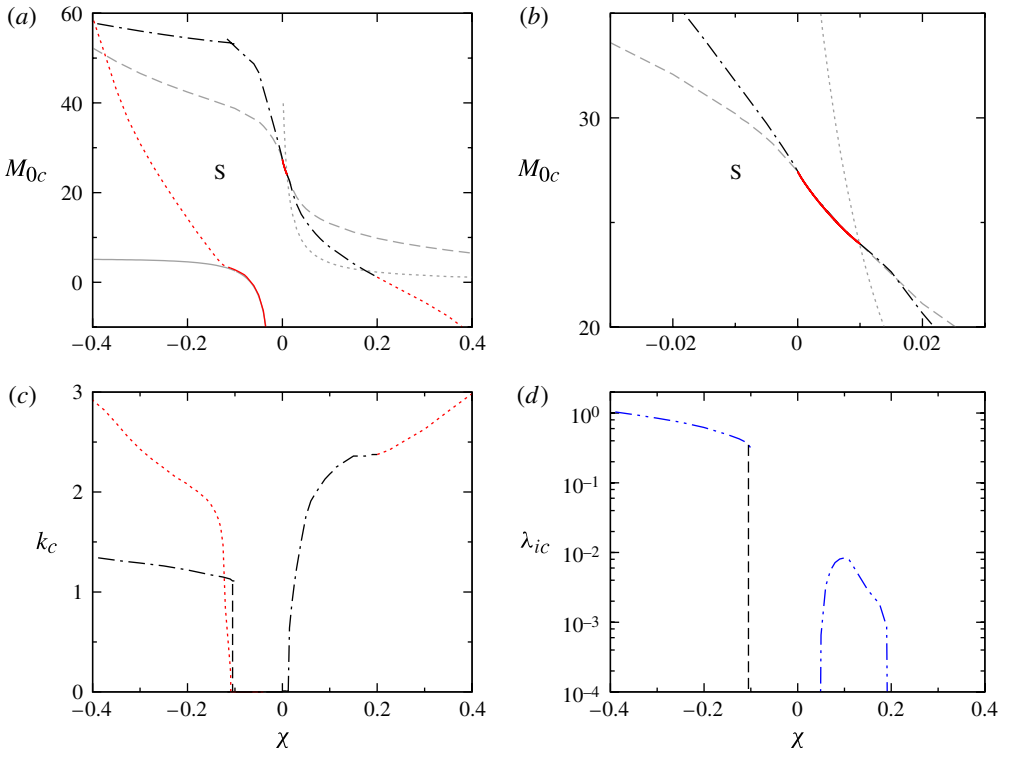


FIGURE 4. (Colour online) Numerical results at $b = 160$ without noise. (*a*) Stability domains $M_{0c}(\chi)$. The dot-dashed and dotted lines correspond to the stability boundaries for the short-wave quasiperiodic and synchronous modes, respectively; the solid line is for the ILW-S mode. The grey lines are the results obtained in the long-wave approximation: the dashed line corresponds to the stability boundary for the SH mode; the solid and dotted lines correspond to the stability margins for the ILW-S and TLW modes, respectively. The domain of stability is marked 'S'. (*b*) Magnified section (small $|\chi|$) of (*a*). (*c*) Variation of critical wavenumber with χ; the lines are the same as in (*a*). (*d*) The frequency of the critical perturbations for the short-wave quasiperiodic mode. The vertical dashed lines in (*c,d*) indicate the abrupt transition from the short-wave quasiperiodic mode to the ILW-Q mode.

discontinuities in figure 4(*a*) at $\chi \approx -0.106$ reflect the above-mentioned competition between two minima on the neutral stability curves for the quasiperiodic mode: with decreasing $|\chi|$, the LW-Q mode becomes critical within (3.3) instead of the short-wave mode. (Recall that in fact neither of these modes are critical, because of the emergence of SH perturbations.) As for the synchronous mode, there is a continuous transition from a short-wave mode to ILW-S; the latter is approached at $\chi = -0.108$ (see the dotted line in figure 4*c*).

The results presented in this section remain qualitatively similar in a wide range of P and φ. Moreover, the variation of the Prandtl number does not lead to visible quantitative changes.

4.2. *Finite level of noise*

Now we proceed to consideration of the finite level of noise (see the dashed line in figure 1*a*); the stability threshold $M_\infty(k)$ is obtained according to (3.13). As stated above, the problem is equivalent to Rayleigh–Marangoni convection in a layer of

https://doi.org/10.1017/jfm.2012.466 Published online by Cambridge University Press

binary mixture. It should also be noted that further simplification of the problem takes place for the monotonic mode: (i) there is no dependence of the neutral stability curves on P; and (ii) the problem can be reduced to that in a pure liquid as explained below.

4.2.1. *Rayleigh–Marangoni convection in a layer of pure liquid*

For monotonic modes the stability thresholds can be derived from the results for Rayleigh–Marangoni convection in a pure liquid (Bergeon, Henry & Ben Hadid 1995). Indeed, for $\lambda = 0$ from (3.3*b*) and (3.3*c*) one obtains that $C_0 = -\chi(1 + L^{-1})T_0$, and therefore the combinations $b\cos\tau(T_0 + \varphi C_0)$ and $M(T_0 - C_0)$, which present in (3.3*a*) and (3.3*e*), can be rewritten as $(\Phi L^{-1} b\cos\tau)T_0$ and $(\chi_L L^{-1} M)T_0$, respectively. This in turn allows us to reduce the problem (3.3) to that of pure liquid by introducing

$$M_\infty = M_p(R_p)\frac{L}{\chi_L}, \quad R_p = \frac{\Phi}{L} b\cos\tau. \tag{4.4}$$

Here M_p and R_p are the Marangoni and Rayleigh numbers for mixed convection in a layer of pure liquid.

To the best of our knowledge, the data on this classical problem are to some extent incomplete. The stability threshold in the long-wave limit

$$\frac{R_p}{320} + \frac{M_p}{48} = 1 \tag{4.5}$$

was first found by Nield (1977), although the formula $R_p/R_c + M_p/M_c = 1$ was first predicted by Nield (1964) when considering the thermally conductive lower boundary. No short-wave instability has been reported; moreover Chary & Chen (1997) stated that the critical wavenumber always vanishes for this problem.

However, our numerical results depicted in figure 5(*a*) show that the short-wave mode becomes critical if R_p and M_p are of different signs and sufficiently large. Since the transition from a long-wave instability to a short-wave one occurs in a continuous manner, the corresponding critical value of R_p can be predicted within the long-wave approximation; the sign of the k^4-contribution to the growth rate λ vanishes at that point. Indeed, according to the linearized version of (3.24) in Oron & Rosenau (1989), we derive

$$\lambda = \left(\frac{19}{5\,913\,600}R_p^2 + \frac{289}{14\,515\,200}R_pM_p - \frac{47}{20\,160}R_p - \frac{1}{120}M_p + \frac{1}{3}\right)k^4 \tag{4.6}$$

exactly at the stability boundary determined by (4.5).

Along the line (4.5), the expression in brackets is negative (i.e. the long-wave mode is critical) between the points with coordinates $(R_p^{(1)}, M_p^{(1)})$ and $(R_p^{(2)}, M_p^{(2)})$, where

$$R_p^{(1,2)} = \frac{320}{241}(209 \pm \sqrt{210\,694}), \quad R_p^{(1)} \approx 887.0, \quad R_p^{(2)} \approx -332.0, \tag{4.7}$$

$$M_p^{(1)} \approx -85.05, \quad M_p^{(2)} \approx 97.80. \tag{4.8}$$

Beyond this interval (i.e. when R_p and M_p are of opposite signs and their absolute values are sufficiently large), a short-wave instability takes place.

The variation of the critical Marangoni number M_{pc} and wavenumber k_c with R_p is demonstrated in figures 5(*b*) and 5(*c*). The short-wave monotonic mode missed in the previous studies takes place at rather large absolute values of the Rayleigh and Marangoni numbers, when these two dimensionless numbers are of different signs.

https://doi.org/10.1017/jfm.2012.466 Published online by Cambridge University Press

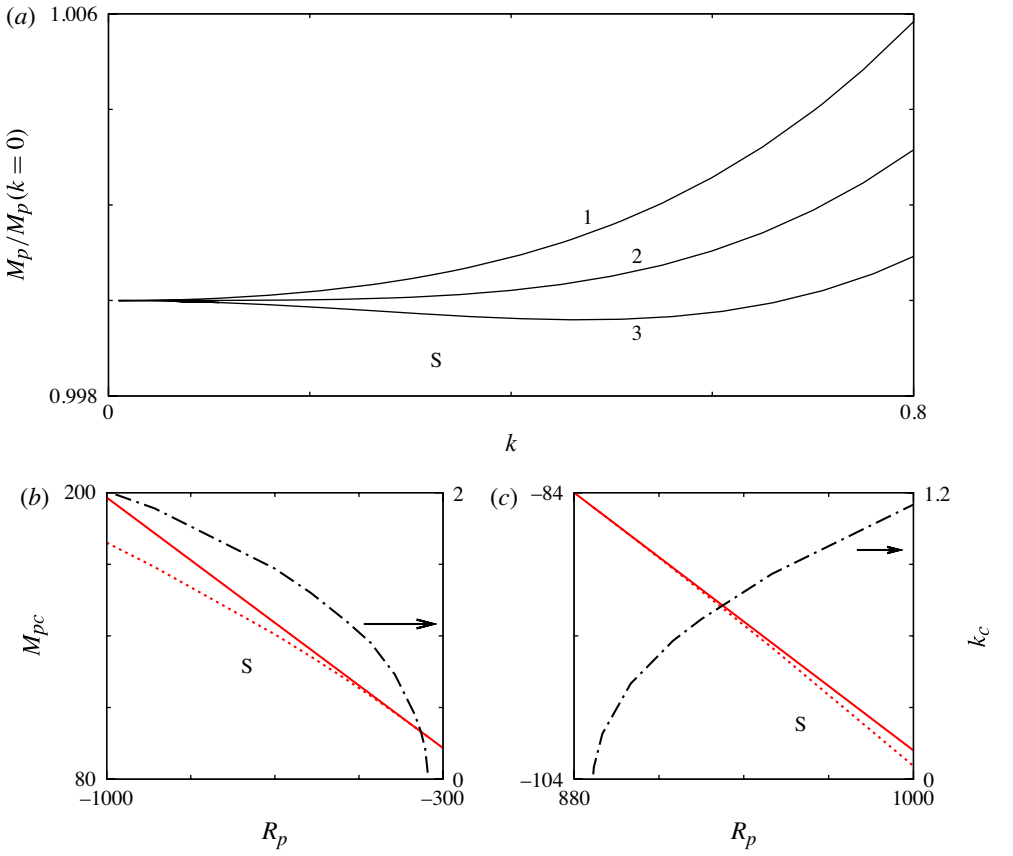


FIGURE 5. (Colour online) Linear stability for Rayleigh–Marangoni convection in a layer of pure liquid; domains of stability are marked 'S'. (*a*) Neutral stability curves 1, 2 and 3 are plotted for $R_p = -300, -332, -360$, respectively. The Marangoni number M_p is normalized with $M_p(k=0)$ given by (4.5). (*b,c*) Variation of the critical Marangoni number M_{pc} (left axes) and wavenumber k_c (right axes, the dot-dashed lines) with the Rayleigh number R_p. In both panels the solid and dashed lines correspond to long-wave and short-wave modes, respectively.

Thus, the effect found is important for such exotic liquids as nematic liquid crystals or molten metals (which have negative σ_T) or for water below 4 °C ($\beta_T < 0$).

4.2.2. *Small k*

Note that for a finite noise level there is no need for a detailed analysis of the long-wave problem, except for the ILW modes. Indeed, with the above-mentioned exception, a long-wave perturbation evolves on a time scale comparable with the period of vibration and there are no long periods of growth and decay. Thus, noise becomes unimportant within the long-wave problem. However, the results for a finite noise intensity should be compared to the remaining long-wave modes (TLW and SH) valid for $\delta = 0$. In all the numerical results given below, the TLW and SH modes are not critical; the short-wave modes for a noisy system win the competition with these two long-wave ones.

An analogue of the ILW modes can be obtained by means of long-wave asymptotics ($k \ll 1$) within (3.3); thus again (4.1) is valid. In contrast to the noise-free system, for

https://doi.org/10.1017/jfm.2012.466 Published online by Cambridge University Press

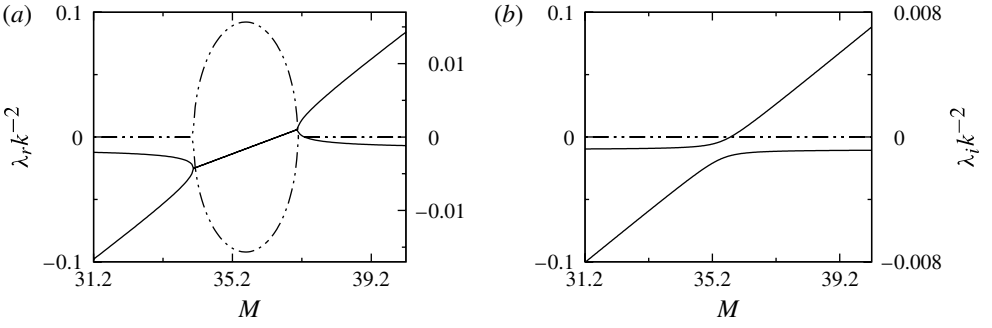


FIGURE 6. Variation of $\lambda_r(\tau=0)/k^2$ and $\lambda_i(\tau=0)/k^2$ with M (the solid and dot-dot-dashed lines, respectively) for the long-wave perturbations in the presence of noise, $b=80$. (*a*) $\chi=-0.0005$, oscillatory mode is critical. (*b*) $\chi=0.0001$, monotonic mode is critical; no oscillatory mode exists.

the finite intensity of noise further simplification is possible. A typical spectrum of perturbations is given in figure 6, where competition between two long-wave modes is clearly seen.

At $\xi_2=0$ a long-wave monotonic (LW-M) mode takes place. The corresponding stability threshold is given by

$$M_\infty^{(m)}=48\frac{L-\Phi A\cos\tau}{\chi_L}. \tag{4.9}$$

(Recall that $A=b/320$, Φ and φ_χ are given below (4.1).) Of course, (4.9) can be obtained from (4.4) and (4.5).

It is obvious that during the period of oscillation $M_\infty^{(m)}$ approaches its minimum or maximum value either at $\tau=0$ or at $\tau=\pi$. Below we discuss only these two cases, referring to the corresponding Marangoni numbers as $M_{\infty+}^{(m)}$ and $M_{\infty-}^{(m)}$, respectively.

At $\xi_1=0$ and $\xi_2<0$ in (4.1), a long-wave oscillatory (LW-O) mode emerges. The critical Marangoni number is given by

$$M_\infty^{(o)}=48\frac{1+L+\varphi_\chi A\cos\tau}{\chi+1}. \tag{4.10}$$

Again, critical perturbations appear at $\tau=0,\pi$; below we refer to the corresponding stability thresholds as $M_{\infty\pm}^{(o)}$. An eigenfrequency is determined by the following expression:

$$\lambda_i=k^2\sqrt{-\frac{\chi(1+L+L^2\mp(1+\varphi)A)+L^2}{1+\chi}}. \tag{4.11}$$

The domains of existence for the oscillatory mode are determined by the positiveness of λ_i^2. The mode takes place at $-1<\chi<\chi_{c\pm}=-L^2/(1+L+L^2\mp(1+\varphi)A)$. (Note that in our calculations $\varphi=1$ and $A\leqslant 1/2$, i.e. no zero value of the denominator is possible.)

The stability boundaries M_∞ in the long-wave limit are plotted in figure 7(*a*); for a fixed sign of $\pm A$ they are qualitatively similar to those found in the absence of the vibration (Oron & Nepomnyashchy 2004). For $\varphi=1$, chosen in computations, $M_{\infty-}^{(o)}>M_{\infty+}^{(o)}$ within the domain of existence of these oscillatory modes $-1<\chi<\chi_{c\pm}$.

https://doi.org/10.1017/jfm.2012.466 Published online by Cambridge University Press

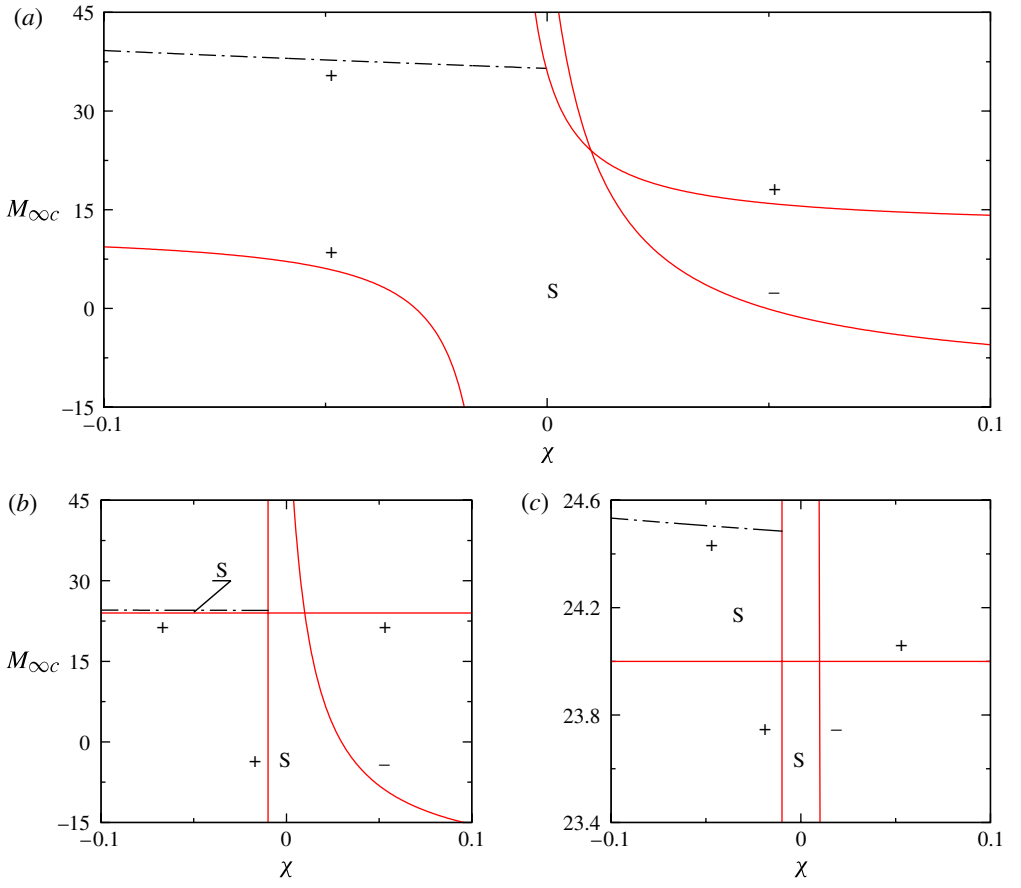


FIGURE 7. (Colour online) Stability domains $M_{\infty c}(\chi)$ for LW modes at a finite level of noise (marked 'S'). The solid and dot-dashed lines correspond to the LW-M (given by (4.9)) and LW-O (given by (4.10)) modes, respectively. (*a*) $b = 80$; (*b*) $b = 160$; (*c*) magnified section of (*b*). Curves marked '+' and '−' are shown for critical perturbations at $\tau = 0$ and $\tau = \pi$, respectively.

Thus, for the oscillatory mode the critical value of the Marangoni number is always reached at $\tau = 0$.

For most of the calculations we set $b = 160$ ($A = 1/2$), varying χ and M. However, for $A\cos\tau = 1/2$ and $\varphi = 1$ the stability boundary given by (4.9) degenerates into a pair of straight lines:

$$\chi_{\infty+}^{(m)} = -\frac{L}{1+L} \quad \text{or} \quad M_{\infty+}^{(m)} = 24. \tag{4.12}$$

The corresponding domains of stability are shown in figures 7(*b*) and 7(*c*).

4.2.3. *Finite k*

For finite k numerical computations are performed. In fact, one has to study only oscillatory modes, whereas the neutral stability curves for the monotonic modes can be recast on the basis of figure 5 and (4.4).

https://doi.org/10.1017/jfm.2012.466 Published online by Cambridge University Press

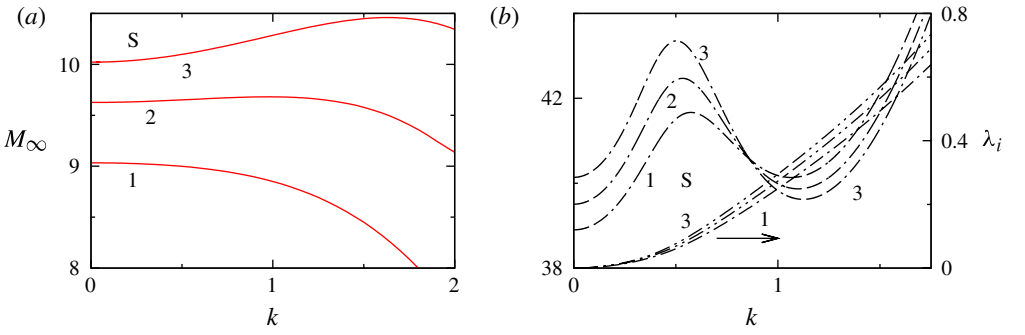


FIGURE 8. (Colour online) Neutral stability curves $M_\infty(k)$ for a noisy system at $b = 80$; lines 1, 2 and 3 correspond to $\chi = -0.09$, -0.11 and -0.13, respectively. The domains of stability are marked 'S'. (*a*) Monotonic mode. (*b*) Oscillatory mode. The dot-dot-dashed lines (right axis) show the variation of the frequency of the neutral perturbations.

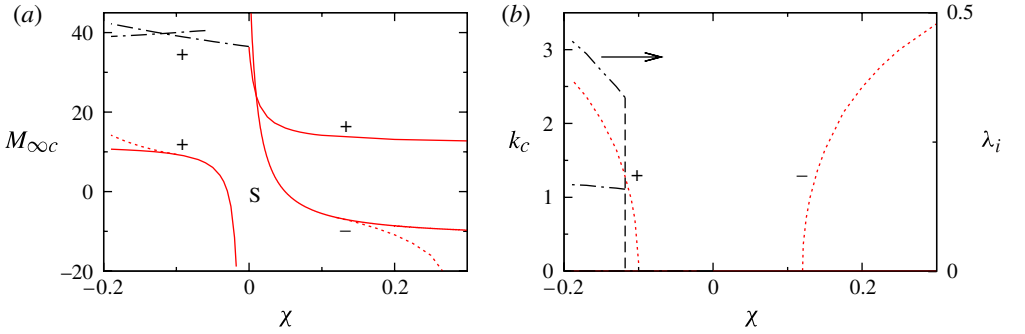


FIGURE 9. (Colour online) Numerical results for finite noise at $b = 80$. (*a*) The domain of stability in the plane $\chi - M_{\infty c}$ is marked 'S'. The solid lines are the stability boundaries for the LW-M mode; the dotted line corresponds to the short-wave monotonic mode, the dot-dashed lines are plotted for either the LW-O mode (at smaller $|\chi|$) or the short-wave oscillatory mode (at larger $|\chi|$). (*b*) The critical wavenumber (left axis, the lines are the same as in *a*) and frequency (right axis, the dot-dot-dashed lines) for the short-wave modes. The vertical dashed line corresponds to the switching between the short-wave oscillatory and LW-O modes.

In figure 8 neutral stability curves are presented at $b = 80$ and three values of the Soret number. Similarly to the system without noise (see figure 2*a*), the domain of stability is confined by the neutral stability curve for the oscillatory mode from above and by that for the monotonic mode from below. The origins of these modes are the same as discussed in § 4.1. It is clearly seen that again competition between long-wave and short-wave modes occurs at negative χ. For both the monotonic and oscillatory modes, at higher $|\chi|$ the critical perturbations belong to the short-wave parts of the neutral stability curves, whereas at smaller $|\chi|$ the LW-O (at $\chi > -0.118$) and LW-M (at $\chi > -0.0999$) modes are critical. The latter value corresponds to $R_p = R_p^{(1)} = 887.0$ and $\tau = 0$ in (4.4).

This competition is also shown in figure 9, where the results of minimization of $M_\infty(k)$ are presented. For the monotonic mode the transition from long-wave to short-wave instability is continuous according to § 4.2.1, whereas for the oscillatory

https://doi.org/10.1017/jfm.2012.466 Published online by Cambridge University Press

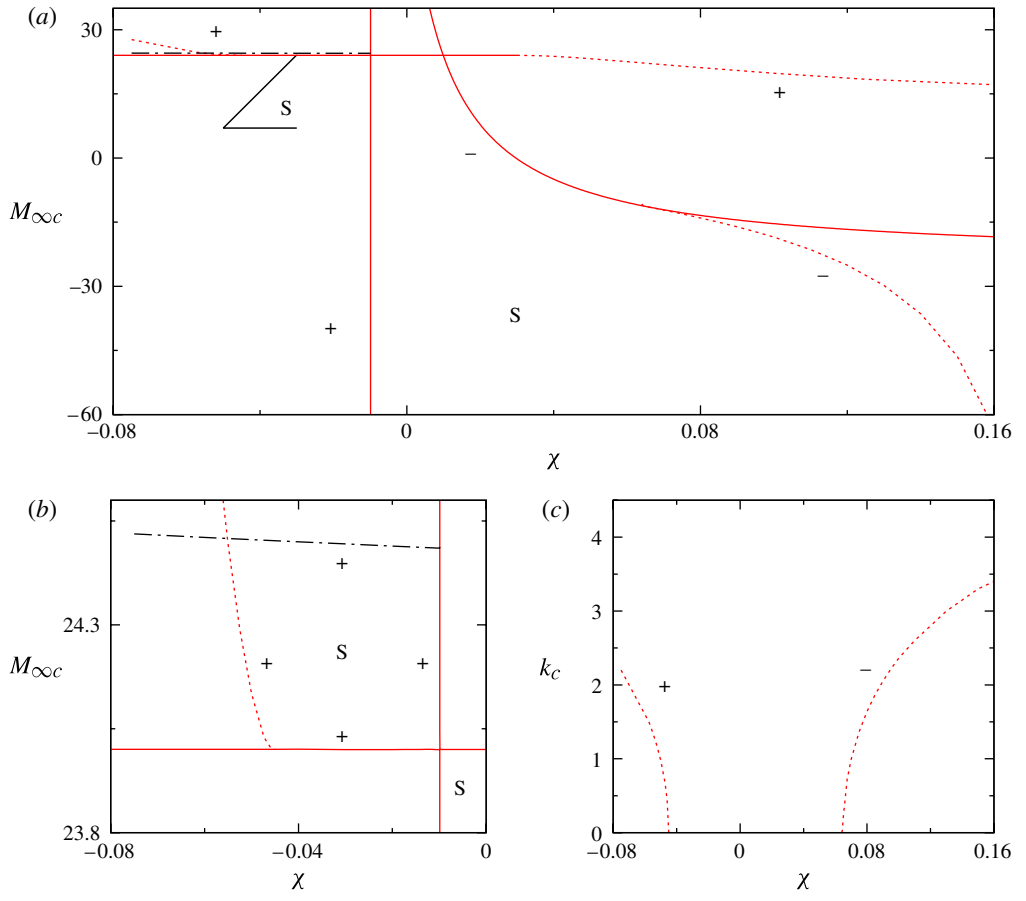


FIGURE 10. (Colour online) Numerical results for a finite level of noise at $b = 160$. The dot-dashed lines correspond to the stability boundary for the LW-O mode; the dotted lines depict the short-wave monotonic mode; the solid lines are for the LW-M mode. (*a*) Stability domains $M_{\infty c}(\chi)$, marked 'S'. For the curves marked '+' ('−'), (3.13) is satisfied at $\tau = 0$ ($\tau = \pi$, respectively), determining neutral stability. (*b*) A magnified section of (*a*). (*c*) Critical wavenumber for the short-wave monotonic mode.

mode the critical wavenumber changes abruptly at $\chi = -0.118$ (see figure 9*b*). Of course, at the same value of the Soret number, the intersection of two dot-dashed lines in figure 9(*a*) occurs. For positive χ, the LW-M mode alternates with the short-wave mode at $\chi = 0.120$, which now corresponds to $R_p = 887.0$ and $\tau = \pi$ in (4.4).

The stability domain in the plane $(\chi, M_{\infty c})$ shown in figure 9(*a*) is qualitatively similar to that without noise (see figure 4*a*). Two main distinctions can be mentioned comparing these figures. First, at $b = 80$, even in the presence of noise, there is no full destabilization of the layer at negative χ. Secondly, in contrast to the noise-free system, where quasiperiodic modes are not critical for negative χ, at a finite level of noise the LW-O mode is critical within a certain interval of the Soret number.

Further increase in b drastically diminishes the stability region: see figure 10(*a*), where the stability domain in the plane $(\chi, M_{\infty c})$ at $b = 160$ is presented. This effect is mainly caused by the considerable destabilization with respect to the long-wave perturbations, shown in figure 7. However, in agreement with (4.4) and (4.7), the

https://doi.org/10.1017/jfm.2012.466 Published online by Cambridge University Press

short-wave mode becomes critical at rather small $|\chi|$, leading to a full destabilization of the layer at negative values of the Soret number. Owing to this fast destabilization no rivalry between short-wave and long-wave oscillatory modes takes place.

Comparing figures 10(*a*) and 4(*a*), one can conclude that the stability region noticeably shrinks in the presence of noise and it is situated at rather small values of the Soret number.

Concluding this subsection, we note that the presented numerical results for the monotonic mode are independent of the Prandtl number. Moreover, our computations demonstrate that the variation of the critical Marangoni number for the oscillatory mode with P is rather small. For instance, for $b = 80$ the neutral stability curves for $P = 10$ cannot be distinguished from the lines presented in figure 8(*b*) on the scale of the plot. Variation of the modified separation number φ is more important. For the monotonic mode, the effect of φ can be taken into account via (4.4); numerical calculations performed for the oscillatory mode at $-0.5 \leqslant \varphi \leqslant 2$ result in 10 % variation in the stability threshold; M_∞ grows slightly as φ increases.

5. Conclusions

The influence of a low-frequency vibration on Marangoni instability in a binary liquid layer is studied within the linear stability problem. Finite values of the perturbation wavenumber are considered by the WKB method.

Neutral stability curves and domains of the stability are obtained in two cases: (i) without noise, i.e. at the margin of neutral stability a module of a multiplier is equal to unity (asymptotic stability); (ii) for a finite level of additive noise (the margin of empirical stability), when a growing perturbation appears at a certain time instant of the vibration period. Depending on the time evolution of the perturbations, short-wave modes fall into two categories: either quasiperiodic or synchronous ones in case (i) and either monotonic or oscillatory in case (ii).

We show that in case (ii) the stability boundaries coincide with those for coupled buoyancy–Marangoni convection in a layer, where the vibration amplitude serves as the Rayleigh number. This problem was analysed by Podolny *et al.* (2008, 2010), but we perform additional calculations to have the results obtained according to both criteria at the same parameter set. Moreover, for the monotonic modes further simplification is possible, and the problem can be reduced to Rayleigh–Marangoni convection in a layer of pure liquid. We have shown that a short-wave monotonic mode was missed in previous studies.

The short-wave modes play an important role for larger values of $|\chi|$ (χ is the Soret number). In particular, no stability is found at negative χ less than some critical value. In contrast, at smaller $|\chi|$ the stability boundary is determined by long-wave modes. In case (i) either the synchronous or SH modes are critical (Fayzrakhmanova *et al.* 2010), and in case (ii) long-wave oscillatory and monotonic modes compete.

Thus, the present paper points out the domain of validity for the long-wave analysis (Fayzrakhmanova *et al.* 2010). Another important issue is a strong destabilization of the layer by low-frequency vibration, especially pronounced when noise is taken into account.

Summarizing both papers, the present one and Fayzrakhmanova *et al.* (2010), we can conclude that a low-frequency external action imposed on a system which possesses a long-wave oscillatory mode results in several striking consequences. In particular, the conventional classifications of perturbations according to their wavenumber (long-wave versus short-wave) and according to a temporal evolution

https://doi.org/10.1017/jfm.2012.466 Published online by Cambridge University Press

(subharmonic, synchronous and quasiperiodic) become coupled and even incomplete. First, two different long-wave synchronous modes take place, TLW and ILW. Secondly, the synchronous short-wave mode can in fact be either synchronous or quasiperiodic or subharmonic, depending on subtle details of the solution of the $O(\omega)$ problem. Third, with the exception just mentioned, subharmonic modes can only be long-wave. Finally, similarly to most systems under low-frequency action, Floquet theory is not sufficient; additive noise of magnitude δ becomes important at $\delta \sim \exp(-\omega^{-1})$.

Acknowledgements

We are grateful to B. Maryshev for a fruitful discussion. The authors acknowledge the support of the Israel Science Foundation (grant 680/10). The work is also supported by the European Union via FP7 Marie Curie scheme Grant PITN-GA-2008-214919 (MULTIFLOW).

Appendix A. Evolution of perturbations near $\tau = \tau_b$ in Case II

Let us consider a simplification of the stability problem at $\tau = \tau_b$, when, as shown in figure 1(*b*), the pair of complex conjugate growth rates splits into two real branches. Near this time instant, $(\lambda - \lambda_0)^2 \approx \Lambda(\tau - \tau_b)$, where the real constants λ_0 and Λ are determined numerically. Dealing only with the lower branch of the spectrum of perturbations, we restore the evolutionary equation for a certain amplitude function $\tilde{f}$ as follows:

$$\frac{\mathrm{d}^2\tilde{f}}{\mathrm{d}t^2} - 2\lambda_0\frac{\mathrm{d}\tilde{f}}{\mathrm{d}t} + \lambda_0^2\tilde{f} - \Lambda\omega(t - t_b)\tilde{f} = 0. \tag{A 1}$$

Upon a substitution $\tilde{f} = \hat{f}\exp(\lambda_0 t)$ and a time rescaling $\hat{t} = (\Lambda\omega)^{1/3}(t - t_b)$, one arrives at the Airy equation:

$$\frac{\mathrm{d}^2\hat{f}}{\mathrm{d}\hat{t}^2} - \hat{t}\hat{f} = 0. \tag{A 2}$$

Since $\hat{t} \sim \omega^{-3/2}(\tau - \tau_b)$ and $\omega \ll 1$, this variable varies from $-\infty$ to ∞, when τ is close to τ_b. Thus, the oscillatory solution

$$\hat{f} = (-\hat{t})^{-1/4}\sin\left(\frac{2}{3}(-\hat{t})^{3/2} + \frac{\pi}{4} + \phi\right) \tag{A 3}$$

at $-\hat{t} \gg 1$ is transformed to the following superposition of growing and decaying functions:

$$\hat{f} \sim \hat{t}^{-1/4}\left(\sin\phi\exp\left(\frac{2}{3}\hat{t}^{3/2}\right) + \frac{\cos\phi}{2}\exp\left(-\frac{2}{3}\hat{t}^{3/2}\right)\right) \tag{A 4}$$

at $\hat{t} \gg 1$. Therefore, the weight factor for the growing solution is given by $\mu = \sin\phi$.

Appendix B. Evolution of perturbations near the intersection of λ_r in Case III

Let us consider the equation valid near $\tau = \tau_c$ in Case III (see figure 1*c*), when the pair of growth rates is given by $\lambda_{1,2} = \lambda_0 \pm \Lambda(\tau - \tau_c) \pm \mathrm{i}\beta$, where λ_0 is complex and both real Λ ($\Lambda > 0$) and β are of order unity. Therefore, the ordinary differential

https://doi.org/10.1017/jfm.2012.466 Published online by Cambridge University Press

equation, governing the dynamics of perturbations near $\tau = \tau_c$, is

$$\frac{\mathrm{d}^2\tilde{f}}{\mathrm{d}t^2} - 2\lambda_0\frac{\mathrm{d}\tilde{f}}{\mathrm{d}t} + \lambda_0^2\tilde{f} - (\Lambda\omega(t - t_c) + \mathrm{i}\beta)^2\tilde{f} = 0. \tag{B 1}$$

Our purpose is to find out whether or not the coupling between the '−' mode (critical at $\tau < \tau_c$) and the '+' mode (critical at $\tau > \tau_c$) exists.

Upon substitution of $\tilde{f} = \bar{f}\exp(\lambda_0 t)$ and replacement of $\bar{t} = \sqrt{\omega}(t - t_c)$, we arrive at

$$\frac{\mathrm{d}^2\bar{f}}{\mathrm{d}\bar{t}^2} - (\bar{t} + \mathrm{i}B)^2\bar{f} = 0, \tag{B 2}$$

where $B = \beta/\sqrt{\omega}$. At $B = 0$, which corresponds to small β and is valid near the point of full intersection of two branches of the complex growth rate, (B 2) coincides with the Schrödinger equation for a quantum oscillator. It is well known that there are no bound states with zero energy for the quantum oscillator. This means that the solution decaying as $\bar{t} \to -\infty$ grows at large positive $\bar{t}$ and vice versa; in other words, the solution, which grows (as $\bar{t}$ increases) at $\bar{t} < 0$ continues to grow at positive $\bar{t}$, i.e. a coupling between two different WKB modes occurs. In contrast, for the robust case of finite β or large B no coupling exists, the solution, which grows at negative $\bar{t}$, starts to decay at $\bar{t} > 0$ and vice versa.

In order to check this conclusion, we also considered a model equation, which gives rise to similar intersection of two real parts of the growth rates at $t = 0, \pi$:

$$\frac{\mathrm{d}^2 f}{\mathrm{d}t^2} - \Omega^2(\sin t + \mathrm{i})^2 f = 0, \tag{B 3}$$

where $\Omega \gg 1$. Our numerical solution via Floquet theory demonstrates that the leading ($O(\Omega)$) order of the Floquet exponent vanishes at large Ω. This result also confirms the conclusion that no interaction of different WKB modes takes place. Indeed, according to WKB theory $\lambda = \pm(\sin t + \mathrm{i})$ and absolute values of both the multipliers are equal to unity.

Thus, the interaction of different WKB modes is absent in the leading order; to gain such interaction one has to go beyond the WKB approximation (Rabinovich & Trubetskov 1989).

REFERENCES

BERGEON, A., HENRY, D. & BEN HADID, H. 1995 Analytical linear stability analysis of Marangoni instability with Soret effect. *Microgravity Q.* **5**, 123–129.

BESTEHORN, M. & BORCIA, I. D. 2010 Thin film lubrication dynamics of a binary mixture: example of an oscillatory instability. *Phys. Fluids* **22**, 104102.

CHARY, M.-I. & CHEN, C.-C. 1997 Onset of stationary Bénard–Marangoni convection in a fluid layer with variable surface tension and viscosity. *J. Phys.* D **30**, 3286–3295.

FAYZRAKHMANOVA, I. S., SHKLYAEV, S. & NEPOMNYASHCHY, A. A. 2010 Influence of a low frequency vibration on a long-wave Marangoni instability in a binary mixture with the Soret effect. *Phys. Fluids* **22**, 104101.

FAYZRAKHMANOVA, I. S., SHKLYAEV, S. & NEPOMNYASHCHY, A. A. 2011 Longwave Marangoni instability in a binary mixture under the action of vibration: influence of the heat transfer on a free surface. *Eur. Phys. J. Special Topics* **192**, 95–100.

FINUCANE, R. G. & KELLY, R. E. 1976 Onset of instability in a fluid layer heated sinusoidally from below. *Intl J. Heat Mass Transfer* **19**, 71–85.

GERSHUNI, G. Z. & LYUBIMOV, D. V. 1998 *Thermal Vibrational Convection*. Wiley.

https://doi.org/10.1017/jfm.2012.466 Published online by Cambridge University Press

HOMSY, G. M. 1974 Global stability of time-dependent flows. Part 2. Modulated fluid layers. *J. Fluid Mech.* **62**, 387–403.

LYUBIMOV, D. V., LYUBIMOVA, T. P. & MARYSHEV, B. S. 2010 Noise effect on convection generation in a modulated gravity field. *Fluid Dyn.* **45**, 859–865.

LYUBIMOVA, T. P. & PARSHAKOVA, Y. N. 2007 Stability of equilibrium of a double-layer system with a deformable interface and a prescribed heat flux on the external boundaries. *Fluid Dyn.* **42**, 695–703.

MYZNIKOVA, B. I. & SMORODIN, B. L. 2001 Convective instability of a horizontal binary-mixture layer in a modulated external force field. *Fluid Dyn.* **36**, 1–19.

MYZNIKOVA, B. I. & SMORODIN, B. L. 2009 Longwave instability of a binary mixture flow in a vertical channel in the presence of vibration. *Fluid Dyn.* **44**, 240–249.

NAYFEH, A. H. 1973 *Perturbation Methods*. Wiley.

NEPOMNYASHCHY, A. A. & SIMANOVSKII, I. B. 2007 Marangoni instability in ultrathin two-layer films. *Phys. Fluids* **19**, 122103.

NIELD, D. A. 1964 Surface tension and buoyancy effects in cellular convection. *J. Fluid Mech.* **19**, 341–352.

NIELD, D. A. 1977 Onset of convection in a fluid layer overlying a layer of a porous medium. *J. Fluid Mech.* **81**, 513–522.

OR, A. C. 2001 Onset condition of modulated Rayleigh–Bénard convection at low frequency. *Phys. Rev.* E **64**, 050201(R).

ORON, A. & NEPOMNYASHCHY, A. A. 2004 Long-wavelength thermocapillary instability with the Soret effect. *Phys. Rev.* E **69**, 016313.

ORON, A. & ROSENAU, P. 1989 Evolution of the coupled Bénard–Marangoni convection. *Phys. Rev.* A **39**, 2063–2069.

PISMEN, L. 1988 Selection of long-scale oscillatory convective patterns. *Phys. Rev.* A **38**, 2564–2572.

PODOLNY, A., ORON, A. & NEPOMNYASHCHY, A. A. 2005 Long-wave Marangoni instability in a binary-liquid layer with deformable interface in the presence of Soret effect: linear theory. *Phys. Fluids* **17**, 104104.

PODOLNY, A., ORON, A. & NEPOMNYASHCHY, A. A. 2006 Linear and nonlinear theory of longwave Marangoni instability with the Soret effect at finite Biot numbers. *Phys. Fluids* **18**, 054104.

PODOLNY, A., NEPOMNYASHCHY, A. A. & ORON, A. 2008 Long-wave coupled Marangoni–Rayleigh instability in a binary liquid layer in the presence of the Soret effect. *Math. Model. Nat. Phenom.* **3**, 1–26.

PODOLNY, A., NEPOMNYASHCHY, A. A. & ORON, A. 2010 Rayleigh–Marangoni instability of binary fluids with small Lewis number and nano-fluids in the presence of the Soret effect. *Fluid Dyn. Mater. Process.* **6**, 13–39.

RABINOVICH, M. I. & TRUBETSKOV, D. I. 1989 *Oscillations and Waves*. Springer.

ROSENBLAT, S. & HERBERT, D. M. 1970 Low-frequency modulation of thermal instability. *J. Fluid Mech.* **43**, 385–398.

SHKLYAEV, S., KHENNER, M. & ALABUZHEV, A. A. 2010 Oscillatory and monotonic modes of long-wave Marangoni convection in a thin film. *Phys. Rev.* E **82**, 025302(R).

SHKLYAEV, S., KHENNER, M. & ALABUZHEV, A. A. 2012 Long-wave Marangoni convection in a thin film heated from below. *Phys. Rev.* E **85**, 016328.

SHKLYAEV, S., NEPOMNYASHCHY, A. A. & ORON, A. 2009 Marangoni convection in a binary liquid layer with Soret effect at small Lewis number: linear stability analysis. *Phys. Fluids* **21**, 054101.

SMORODIN, B. L., MYZNIKOVA, B. I. & KELLER, I. O. 2002 On the Soret-driven thermosolutal convection in a vibrational field of arbitrary frequency. *Lect. Notes Phys.* **584**, 372–388.

https://doi.org/10.1017/jfm.2012.466 Published online by Cambridge University Press